Article

A Delicate Electronic Balance between Metal and Ligand in [Cu–P–Cu–P] Diamondoids: Oxidation State Dependent Plasticity and the Formation of a Singlet Diradicaloid

Young Min Rhee, and Martin Head-Gordon

J. Am. Chem. Soc., **2008**, 130 (12), 3878-3887 • DOI: 10.1021/ja0764916

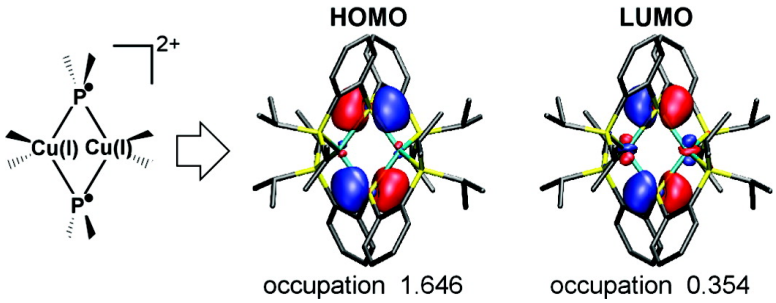

More About This Article

Additional resources and features associated with this article are available within the HTML version:

- Supporting Information
- Access to high resolution figures
- Links to articles and content related to this article
- Copyright permission to reproduce figures and/or text from this article

View the Full Text HTML

J|A|C|S
ARTICLES
Published on Web 03/04/2008

A Delicate Electronic Balance between Metal and Ligand in [Cu−P−Cu−P] Diamondoids: Oxidation State Dependent Plasticity and the Formation of a Singlet Diradicaloid

Young Min Rhee and Martin Head-Gordon*

Department of Chemistry, University of California, and Chemical Sciences Division, Lawrence Berkeley National Laboratory, Berkeley, California 94720

Received August 28, 2007; E-mail: mhg@cchem.berkeley.edu

Abstract: Transition metal atoms often participate in redox reactions as catalytic sites, where ligand groups play an important role in orchestrating catalytic activity, especially in metalloenzymes. A major issue is to understand connections between oxidation state and geometry at the metal center, because geometric reorganization is directly related to reaction rate. In this article, we analyze an intriguing oxidation-induced geometrical change in [Cu−P−Cu−P] ring structures (~0.6 Å change in metal−metal distance) using quantum chemical approaches. We find that the Cu−P interactions in the ring of the neutral species consist of four localized P → Cu dative bonds. Successive oxidations extract electrons predominantly from P atoms on the ring rather than Cu sites. It emerges that as a result, the Cu−P interactions change and also exhibit partial Cu(3d) → P donation, which causes the large distortion in geometry. We also find that the dication possesses a large degree of diradical character, forming a rare example of an observed species that is a singlet diradicaloid. This hypothesis is supported by our computational results as well as previously reported experimental features.

1. Introduction

Metal atoms and their ions play crucial roles in many redox enzymes, which are essential in various metabolic processes.[1] One of the most important features of such metalloenzymes is their structural variations in the ligand group bindings. Often related to the old architectural technique of entasis,[2] it has been long believed that enzymes can fine-tune the redox potentials of their metal atoms, and thus their catalytic activity, through the use of distorted ligating structures controlled by the surrounding protein matrix.[2,3] Of the many transition metal species, copper has been studied extensively[4−12] in this context because it adopts fundamentally different coordination geometries depending on its oxidation states (usually, tetragonal for Cu(II) versus tetrahedral for Cu(I)).[11] In fact, this characteristic of copper appears to be utilized in various enzymes with rapid long-range electron-transfer capabilities.[1,13]

Recently, a new view has arisen regarding the nature of the active copper sites in metalloenzymes. Through the use of X-ray absorption spectroscopy and electronic structure calculations, Solomon and co-workers have suggested that active site covalent bonds involving the metal atoms may determine the reactivity of the enzymes.[13−16] In addition, theoretical investigations by Ryde and co-workers using model molecules to represent blue copper protein have also shown that the small reorganization energy[17] (and thus the high electron-transfer rate) in the enzyme originates from the nature of copper to sulfur bonding and not from steric constraints imposed by the protein.[18,19]

Even though the distinction between the geometric and electronic control of the entatic state[12] may appear to be somewhat semantic because the variation in geometry and the change in covalency are tightly interconnected, it still has an important practical implication for studies of metalloenzymes and related systems. Indeed, numerous efforts have been devoted to the development of small biomimetic molecules over the past

(1) Karlin, K. D. *Science* **1993**, *261*, 701.
(2) Vallee, B. L.; Williams, R. J. P. *Proc. Natl. Acad. Sci. U.S.A.* **1968**, *59*, 498.
(3) Williams, R. J. P. *Inorg. Chim. Acta Rev.* **1971**, *5*, 137.
(4) Norris, G. E.; Anderson, B. F.; Baker, E. N. *J. Am. Chem. Soc.* **1986**, *108*, 2784.
(5) Guss, J. M.; Freeman, H. C. *J. Mol. Biol.* **1983**, *169*, 521.
(6) Petratos, K.; Banner, D. W.; Beppu, T.; Wilson, K. S.; Tsernoglou, D. *FEBS Lett.* **1987**, *218*, 209.
(7) Baker, E. N. *J. Mol. Biol.* **1988**, *203*, 1071.
(8) Adman, E. T.; Turley, S.; Bramson, R.; Petratos, K.; Banner, D.; Tsernoglou, D.; Beppu, T.; Watanabe, H. *J. Biol. Chem.* **1989**, *264*, 87.
(9) Hart, P. J.; Nersissian, A. M.; Herrmann, R. G.; Nalbandyan, R. M.; Valentine, J. S.; Eisenberg, D. *Protein Sci.* **1996**, *5*, 2175.
(10) Guss, J. M.; Merritt, E. A.; Phizackerley, R. P.; Freeman, H. C. *J. Mol. Biol.* **1996**, *262*, 686.
(11) Rorabacher, D. B. *Chem. Rev.* **2004**, *104*, 651.
(12) Chaka, G.; Sonnenberg, J. L.; Schlegel, H. B.; Heeg, M. J.; Jaeger, G.; Nelson, T. J.; Ochrymowycz, L. A.; Rorabacher, D. B. *J. Am. Chem. Soc.* **2007**, *129*, 5217.
(13) Solomon, E. I.; Lowery, M. D. *Science* **1993**, *259*, 1575.
(14) Solomon, E. I.; Randall, D. W.; Glaser, T. *Coord. Chem. Rev.* **2000**, *200*, 595.
(15) Solomon, E. I.; Szilagyi, R. K.; George, S. D.; Basumallick, L. *Chem. Rev.* **2004**, *104*, 419.
(16) Williams, K. R.; Gamelin, D. R.; LaCroix, L. B.; Houser, R. P.; Tolman, W. B.; Mulder, T. C.; de Vries, S.; Hedman, B.; Hodgson, K. O.; Solomon, E. I. *J. Am. Chem. Soc.* **1997**, *119*, 613.
(17) Marcus, R. A.; Sutin, N. *Biochim. Biophys. Acta* **1985**, *811*, 265.
(18) Ryde, U.; Olsson, M. H. M.; Pierloot, K.; Roos, B. O. *J. Mol. Biol.* **1996**, *261*, 586.
(19) Olsson, M. H. M.; Ryde, U.; Roos, B. O. *Protein Sci.* **1998**, *7*, 2659.

10.1021/ja0764916 CCC: $40.75

Table 1. Definitions of Basis Sets and Their Contraction Schemes Adopted in This Work

	atoms[a]		
designatn	C	P	Cu
D:TP	6-31G (10s4p)/[3s2p]	6-311G(d) (13s9p1d)/[6s5p1d]	Wachters+f (14s11p6d3f)/[8s6p4d1f]
TP:TP	6-311G(d) (11s5p1d)/[4s3p1d]	6-311G(d) (13s9p1d)/[6s5p1d]	Wachters+f (14s11p6d3f)/[8s6p4d1f]
D:T3P	6-31G (10s4p)/[3s2p]	6-311G(3d) (13s9p3d)/[6s5p3d]	Wachters+3f[b] (14s11p6d3f)/[8s6p4d3f]
D:T(+)P	6-31G (10s4p)/[3s2p]	6-311+G(d) (14s10p1d)/[7s6p1d]	Wachters+f (14s11p6d3f)/[8s6p4d1f]
D:T(+)3P	6-31G (10s4p)/[3s2p]	6-311+G(3d) (14s10p3d)/[7s6p3d]	Wachters+3f[b] (14s11p6d3f)/[8s6p4d3f]
D:T(2+)3P	6-31G (10s4p)/[3s2p]	6-311(2+)G(3d) (15s11p3d)/[8s7p3d]	Wachters+3f[b] (14s11p6d3f)/[8s6p4d3f]
D:TZVPP	6-31G (10s4p)/[3s2p]	TZVPP (14s9p2d1f)/[5s5p2d1f]	TZVPP (17s11p6d1f)/[6s4p3d1f]

[a] For hydrogens, the 6-31G basis was used in all cases. [b] Wachters+3f is defined by uncontracting three primitive f-functions in Wachters+f.

few decades.[20] The design principles for metalloenzyme mimics should come from fundamental understanding of the mechanistic aspects of the enzymes and will be the basis for development of novel molecules with practical utility. For example, the development of covalency-oriented enzyme mimics involving electronic entatic states[12] should focus on duplicating active site electronic structure, while the geometrically driven design efforts should focus on reproducing the active site geometry.[11]

While the effect of geometrical constraints will be mostly electrostatic (through the ligand field imposed on the metal atoms) or steric, the covalency will also be critically affected by the atoms involved in bond formation. Accordingly, elucidating the bonding of various copper-containing species in relation to their redox properties will be a step toward more general understanding of electron-transfer systems based on transition metals. In this article, we report the result of detailed quantum chemical characterizations of the bonding in [Cu−P−Cu−P] diamondoid species [copper(I) bis(2-(diisopropylphosphino)-phenyl)phosphide]$_2$ (**1**) and its simplified model [$(PH_3)(PH_3)$-$Cu(PH_2)]_2$ (**2**). Recently synthesized and experimentally characterized by Peters and co-workers,[21,22] **1** exhibits an intriguingly large geometric distortion upon oxidation. Explaining the origin of this peculiarity will very likely connect to the redox-dependence of the bonding in the central core defined as the [Cu−P−Cu−P] ring. Comparisons with the simplified model molecule, **2**, will enable additional insights regarding the role of the surrounding ligand groups and the effect of their geometrical constraints.

Quantum chemical methods have been proven to be invaluable for such tasks in various molecular systems. Here, we show that the geometrical changes among **1**/**1**$^+$/**1**$^{2+}$ can be adequately reproduced by conventional quantum chemical calculations, as well as other experimental properties.[21,22] To analyze the bonding, we apply an efficient one-electron orbital localization scheme[23] and deduce that the geometrical distortion is a result of drastic oxidation-induced changes in the bonding within the diamond core. These features are well preserved in the model **2** and its oxidized states, suggesting that they are primarily governed by the metal−ligand bonds in the core. On the basis of the observed bonds and their origin from orbital interactions, we reason that the peculiar characteristics of this system originate from its delicate "electronic balance" between the metal and the ligand atoms. Finally, we predict that the exotic bonds in the diamond core of the system will lead to spatially separated partially unpaired electrons in the dication, forming a rare singlet diradicaloid species[24−27] as an isolatable chemical entity. Further implications of these results are also discussed at the conclusion of this work.

2. Methods

2.1. Geometry Optimization and Basis Set Dependence. For this diamondoid system, the most straightforward way to present the dependence of the geometries on its oxidation states will be to obtain the molecular energies as a function of geometric distortion in the diamond core after each step of oxidation. Even though such calculations are computationally rather expensive, they can furnish more information than simple globally optimized geometries. Such potential energy surfaces (PES's) were calculated in **1**/**1**$^+$/**1**$^{2+}$ with constrained geometry optimizations[28] using density functional theory (DFT).[29] The Cu−Cu distance was used as the constraint parameter to explore the energetic price of core distortion. DFT calculations were performed using the exchange functional of Becke[30] and the correlation functional of Perdew,[31] a combination commonly known as BP86. The exchange-correlation integrals were evaluated with an efficient and reliable standard quadrature grid (SG-1).[32] The system was found to have negligible dependence on the choice of the exchange-correlation functional and the inclusion of the relativistic effect from the copper nuclei. Details of these validity checks can be found in the Supporting Information.

Because the [Cu−P−Cu−P] core in the experimental geometry has rather long Cu−P distances (∼2.3 Å), the description of bonding in the core may depend on the adequacy of the basis set. For this reason, we have tried the series of basis sets listed in Table 1. First, for the constrained optimizations, a D:TP mixed basis set was adopted. This basis set describes Cu and P atoms with Wachters+f[33,34] and 6-311G-(d)[35,36] bases, respectively, which are both equal to or better than polarized valence triple-ζ (thus, denoted as "TP"). The detailed contraction scheme from the primitive Gaussian basis functions is also explained in Table 1. For carbon and hydrogen atoms, the relatively small 6-31G basis set was used for computational efficiency. After we obtained optimized structures at each Cu−Cu distance at this BP86/D:TP level, single point energy calculations were performed with different basis sets at each geometry using both lower and higher quality

(20) Holm, R. H.; Solomon, E. I. *Chem. Rev.* **2004**, *104*, 347.
(21) Harkins, S. B.; Mankad, N. P.; Miller, A. J. M.; Szilagyi, R. K.; Peters, J. C. *J. Am. Chem. Soc.* **2008**, *130*, 3478−3485.
(22) Mankad, N. P.; Rivard, E.; Harkins, S. B.; Peters, J. C. *J. Am. Chem. Soc.* **2005**, *127*, 16032.
(23) Subotnik, J. E.; Shao, Y.; Liang, W.; Head-Gordon, M. *J. Chem. Phys.* **2004**, *121*, 9220.
(24) Borden, W. T. *Diradicals*; Wiley-Interscience: New York, 1982.
(25) Borden, W. T.; Iwamura, I.; Berson, J. A. *Acc. Chem. Res.* **1994**, *27*, 109.
(26) Pedersen, S.; Herek, J. L.; Zewail, A. H. *Science* **1994**, *266*, 1359.
(27) Berson, J. A. *Science* **1994**, *266*, 1338.
(28) Baker, J. *J. Comput. Chem.* **1992**, *13*, 240.
(29) Parr, R. G.; Yang, W. *Density-Functional Theory of Atoms and Molecules*; Oxford University Press: New York, 1989.
(30) Becke, A. D. *Phys. Rev. A* **1988**, *38*, 3098.
(31) Perdew, J. P. *Phys. Rev. B* **1986**, *33*, 8822.
(32) Gill, P. M. W.; Johnson, B. G.; Pople, J. A. *Chem. Phys. Lett.* **1993**, *209*, 506.
(33) Wachters, A. J. H. *J. Chem. Phys.* **1970**, *52*, 1033.
(34) Bauschlicher, C. W., Jr.; Langhoff, S. R.; Barnes, L. A. *J. Chem. Phys.* **1989**, *91*, 2399.
(35) Krishnan, R.; Binkley, J. S.; Seeger, R.; Pople, J. A. *J. Chem. Phys.* **1980**, *72*, 650.
(36) McLean, A. D.; Chandler, G. S. *J. Chem. Phys.* **1980**, *72*, 5639.

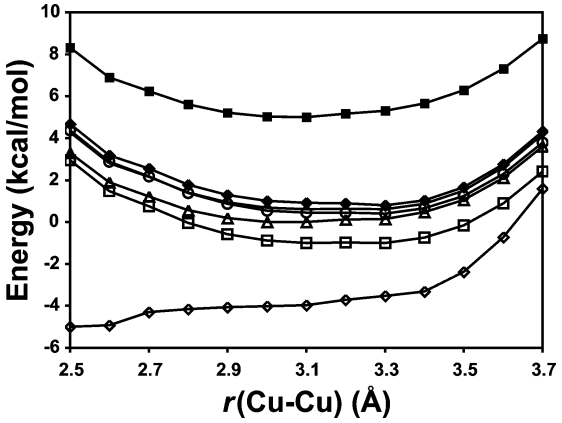

Figure 1. Basis set dependence of the conformational energy surface of **1** as a function of Cu−Cu distance. The adopted basis sets are 6-31G(d), D:TP, TP:TP, D:T(+)P, D:T(+)3P, D:T(2+)3P, and D:TZVPP from the bottom to the top curves (see text for full explanation). The curves are shifted vertically for visual clarity.

bases. The adequacy of using the small basis (6-31G) for carbon was tested by replacing it with 6-311G(d), as denoted by TP:TP in Table 1. The adequacy of the basis on Cu and P atoms was also tested by adding more polarization and/or diffuse functions on these atoms. Finally, the possibility of using a small basis set was examined by using 6-31G(d) on all atoms.

Figure 1 compares the PES's of **1** obtained with these basis sets. Perhaps consistent with a long and diffuse bond between Cu and P, the small double-ζ quality set (6-31G(d)) behaves very differently from others and cannot capture the experimentally observed Cu−Cu distance. Considering that the difference between TP:TP and D:TP surfaces is negligible, we can conclude that the defect of the double-ζ basis is caused by lack of functions on P and Cu atoms. Because all triple-ζ basis sets behave similarly in the description of **1**, we have used the D:TP set for all other constrained geometry optimizations for computational efficiency.

Full geometry optimizations without any constraints were also performed for both **1** and **2** and their cations starting from minimum energy conformations obtained in the constrained optimizations. In these calculations, the highest quality basis set D:T(2+)3P was adopted even though using a smaller set (e.g., D:TP) would not lead to any qualitative difference as can be inferred from Figure 1. These geometries were used in the analyses of molecular properties such as atomic charges and chemical bonding as depicted by localized occupied orbitals.

2.2. Orbital Localization. Canonical orbitals as obtained from standard DFT calculations are usually delocalized in large molecules and, hence, are not the best choice for describing chemical bonding. For this purpose, we transform to localized occupied obitals[37] via the Edmiston−Ruedenberg (ER) scheme,[38] which maximizes the Coulomb self-interaction of the orbitals. Even though the advantage of using local orbitals was known decades ago,[38−41] their practical application has been hindered by high computational cost, especially for the ER scheme. With a recently implemented efficient algorithm for ER localization,[23] we were able to obtain well-converged results with reasonable efficiency. Because the core electrons do not effectively participate in the formation of the chemical bonds, only the valence occupied orbitals were included in the localization process. Carbon 1s, phosphorus 1s/2s/2p, and Cu 1s/2s/2p/3s/3p electrons were considered to occupy the core space, totaling 96 core orbitals in **1** and 48 core orbitals in **2** (and with 158 and 34 valence orbitals in **1** and **2**, respectively).

2.3. Singlet Diradicaloid Character. Even though there are a number of indirect means within DFT to suggest potential diradical character for a system with an even number of electrons, conventional DFT cannot attain a definitive description because the formation of a singlet diradicaloid is a result of partial electron occupations of the antibonding orbitals (often termed as "static correlation"). Such a phenomenon can only be properly described when those occupations are explicitly treated through the use of wave-function-based methods. Accordingly, we have performed perfect pairing (PP)[42] calculations on **1** and its model **2** (neutral and dication) to obtain the antibonding orbital occupations. PP is an efficient and usually reliable replacement of more rigorous but practically intractable treatments such as the complete active-space method.[43] In the calculation of the model system ($\mathbf{2}^{2+}$), all valence orbitals as defined in the localization scheme were first considered to be active in pairing. This resulted in effectively one pair of orbitals with appreciable occupations. When a new PP calculation was carried out with only one active pair, the population and the shape of the optimized pairing orbitals were in good agreement with the results from the pairing in the complete valence space. Thus, for $\mathbf{1}^{2+}$, we consider one pair of active orbitals in the PP calculation for computational efficiency.

In both ER localization and PP calculations, we use the resolution-of-the-identity (or density fitting) approximation[44−50] for efficient evaluation of 4-center 2-electron integrals. For this purpose, the 6-31G basis for carbon and hydrogen is paired with the VDZ fitting basis.[49] For copper and phosphorus, where optimized auxiliary bases corresponding to the 6-311G and Wachters sets are not available, we instead use the TZVPP set[33,51,52] with its corresponding fitting basis.[49] This combination (termed as D:TZVPP) is somewhat smaller than D:T(2+)-3P (see Table 1), but as shown in Figure 1, the D:TZVPP PES is very similar to the D:T(2+)3P surface. In addition, when the smaller 6-31G-(d) basis was used to obtain the local orbital shapes and the PP occupancies, the results were quite similar to the D:TZVPP case. On the basis of both the similarity of its PES to the larger basis result and the weak basis set dependence in those property analyses, one can ascertain that D:TZVPP is an adequate basis set for the localized orbitals and PP calculations. All the calculations were carried out using a development version of the Q-Chem 3.1 package,[53] and the orbital plots were rendered using VMD.[54]

3. Results and Discussion

3.1. Oxidation-Dependent Plasticity. Figure 2 presents the potential energy surfaces for **1**, $\mathbf{1}^{+}$, and $\mathbf{1}^{2+}$ at varying Cu−Cu distances. As can be inferred from the locations of the energy minima, the molecule exhibits large geometrical distortions upon oxidation. Also, the singlet spin state of $\mathbf{1}^{2+}$ is always lower in energy than the triplet state regardless of its geometry. These are in exact accord with experimental observations.[21,22] Another

(37) The adequacy of using local orbitals in describing chemical bonds can be trivially reasoned, and curious readers are referred to the Supporting Information.

(38) Edmiston, C.; Ruedenberg, K. *Rev. Mod. Phys.* **1963**, *35*, 457.
(39) Lennard-Jones, J. E.; Pople, J. A. *Proc. R. Soc. London, Ser. A* **1950**, *202*, 166.
(40) Boys, S. F. *Rev. Mod. Phys.* **1960**, *32*, 296.
(41) Pipek, J.; Mezey, P. G. *J. Chem. Phys.* **1989**, *90*, 4916.
(42) Van Voorhis, T.; Head-Gordon, M. *J. Chem. Phys.* **2000**, *112*, 5633.
(43) Roos, B. O.; Taylor, P. R.; Siegbahn, P. E. M. *Chem. Phys.* **1980**, *48*, 157.
(44) Dunlap, B. I.; Connolly, J. W. D.; Sabin, J. R. *J. Chem. Phys.* **1979**, *71*, 3396.
(45) Whitten, J. L. *J. Chem. Phys.* **1973**, *58*, 4496.
(46) Feyereisen, M.; Fitzgerald, G.; Komornicki, A. *Chem. Phys. Lett.* **1993**, *208*, 359.
(47) Vahtras, O.; Almlöf, J.; Feyereisen, M. W. *Chem. Phys. Lett.* **1993**, *213*, 514.
(48) Werner, H.-J.; Manby, F. R.; Knowles, P. J. *J. Chem. Phys.* **2003**, *118*, 8149.
(49) Weigend, F.; Häser, M.; Patzelt, H.; Ahlrichs, R. *Chem. Phys. Lett.* **1998**, *294*, 143.
(50) Eichkorn, K.; Treutler, O.; Öhm, H.; Häser, M.; Ahlrichs, R. *Chem. Phys. Lett.* **1995**, *240*, 283.
(51) Schäfer, A.; Huber, C.; Ahlrichs, R. *J. Chem. Phys.* **1994**, *100*, 5829.
(52) Woon, D. E.; Dunning, T. H., Jr. *J. Chem. Phys.* **1993**, *98*, 1358.
(53) Shao, Y.; et al. *Phys. Chem. Chem. Phys.* **2006**, *8*, 3172.
(54) Humphrey, W.; Dalke, A.; Schulten, K. *J. Mol. Graphics* **1996**, *14*, 33.

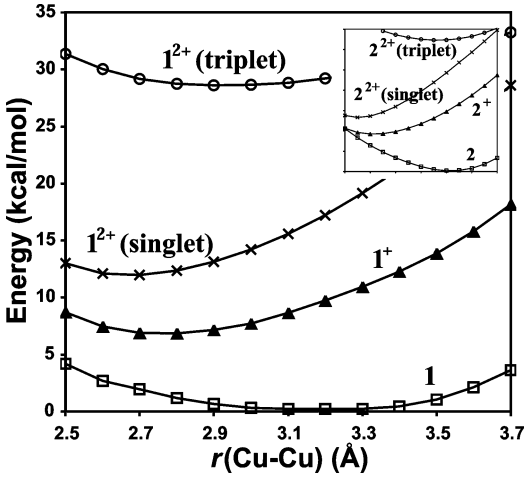

Figure 2. Potential energy surfaces of the diamondoid molecule in three oxidation states at the BP86/D:TP level of theory. The surfaces have been obtained by performing constrained optimizations at each given Cu−Cu distance. For visual clarity, cationic and dicationic surfaces are shifted downward arbitrarily. (The unshifted surfaces can be found in Supporting Information.) The inset shows the surfaces of the simplified model molecule.

Chart 1

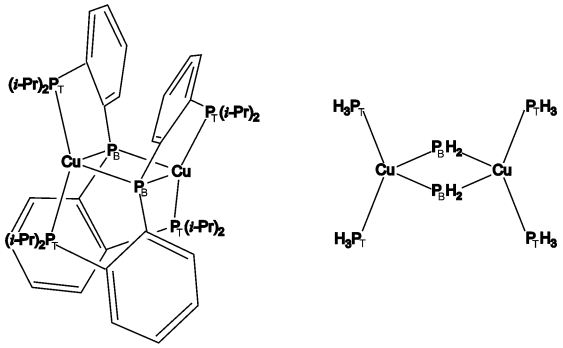

1 **2**

important feature to note in this figure is the fact that all surfaces show rather wide basins around the minima. Accordingly, one can expect that the [Cu−P_B−Cu−P_B] core will be flexible to some degree even at low temperatures (hereafter, P_B and P_T will denote bridging and terminal P atoms as shown in Chart 1). The fully optimized structures at each oxidation state (without any constraints) are in good agreement with experimental parameters as listed in Table 2. The slight discrepancies in the diagonal distances of the diamond cores (r(Cu−Cu) and r(P_B−P_B)) should be expected, considering the flexibility of the core and the difference between the computational (gas phase) and experimental (crystal) environments. Of course, the computationally optimized minimum energy geometry will always be slightly different from the vibrationally averaged experimental geometry even when both are in the gas phase.

Table 2 also presents the charge distributions on the core (ring) atoms and the surrounding P_T atoms as obtained with natural population analysis.[55,56] In the neutral species, the charge population on Cu suggests that its oxidation state will be close to that of Cu(I). Also, from the large difference between populations on bridging and terminal P atoms, we can infer that P_B atoms will carry a large portion of the negative charge in **1** at the neutral state. Most importantly, oxidations predominantly affect P_B atoms, without altering the charge environment on Cu or P_T atoms significantly.

These observations are in good accord with previous experimental findings from both X-ray absorption spectroscopy (XAS) and ^{31}P nuclear magnetic resonance (NMR). Specifically, the copper K-edge absorptions (1s → 4p) of the three differently oxidized species showed very similar spectra, signifying that the charge environment of Cu atoms changes rather little upon oxidation.[21] In addition, the extreme downfield chemical shift (−21.0 ppm with **1** versus 266.1 ppm with $\mathbf{1}^{2+}$) of P_B atoms upon oxidation reported by Peters and co-workers[22] will be the result of their electron loss after oxidation. The change in the chemical shift of P_T atoms is insignificant (34.0 ppm with **1** versus 37.3 ppm with $\mathbf{1}^{2+}$),[22] suggesting that the changes in the electronic environment on these atoms and their adjacent C/Cu atoms are negligible.

Given the above observation that the main oxidation-induced population changes occur on P_B atoms in the diamond core, the next question is whether the rather complicated ligands are playing an essential role in tuning the geometries at different oxidation states. This is the main reason the model system **2** is considered in parallel. Table 2 shows the geometrical parameters of **2** at various oxidation states. Interestingly, this simplified molecule exhibits plasticity that is in close agreement with the behavior of the original system **1**. The somewhat noticeable differences in the bond angles are likely a result of the lack of steric constraints imposed by the bulky "side chains" around P atoms. In fact, while the model systems $\mathbf{2}^{n+}$ possess D_{2h}-like symmetry with near-perfect reflection symmetry against the core plane, the near-core structures of $\mathbf{1}^{n+}$ closely follow D_2 symmetry in both theory and experiment, without the reflection symmetry. Therefore, we can conclude that oxidation-dependent geometrical changes stem from electronic structure within the core, rather than from the side chains of the ligand. (In the experimental situation, of course, the side chains may play the important role of preventing the solvent or adjacent $\mathbf{1}^{n+}$ molecules from disrupting the core.)

The conserved oxidation state of the metal atoms associated with the noninnocent[21,57,58] ligand group is somewhat surprising when one considers the debate regarding geometric or electronic origin of the entatic states in response to oxidation/reduction of the metal center. Given that the effective oxidation state of the metal atoms is always Cu(I), then the preferred coordination around them would likely be preserved even after oxidations. In reality, however, the geometry changes drastically as the molecule is oxidized. On the basis of the similar behavior of **1** and **2**, we can safely assume that this peculiarity is not caused by the characteristics of the ligand. The possibility of electrostatic attraction/repulsion can also be excluded: because the repelling effect of two bridging phosphide groups (partially negative) is removed upon oxidation, r(P_B−P_B) would be shortened if the geometry is governed by the electrostatic interactions. Thus, it is natural to assume that the oxidation induces some changes in the chemical bonding in the core. These

(55) Glendening, E. D.; Badenhoop, J. K.; Reed, A. E.; Carpenter, J. E.; Bohmann, J. A.; Morales, C. M.; Weinhold, F. *NBO 5.0*; Theoretical Chemistry Institute, University of Wisconsin: Madison, WI, 2001.
(56) Szabo, A.; Ostlund, N. S. *Modern Quantum Chemistry: Introduction to Advanced Electronic Structure Theory*; McGraw-Hill: New York, 1989.
(57) Ray, K.; Bill, E.; Weyhermüller, T.; Wieghardt, K. *J. Am. Chem. Soc.* **2005**, *127*, 5641.
(58) Szilagyi, R. K.; Lim, B. S.; Glaser, T.; Holm, R. H.; Hedman, B.; Hodgson, K. O.; Solomon, E. I. *J. Am. Chem. Soc.* **2003**, *125*, 9158.

Table 2. Structural Parameters of the Optimized Geometries of the Diamondoids at Different Oxidation States[a]

param		X	X^+	X^{2+}
geometry[b]	r(Cu−Cu)	3.10/3.33/3.31	2.75/2.73/2.77	2.66/2.60/2.60
	r(P_B−P_B)	3.50/3.31/3.27	3.66/3.74/3.61	3.66/3.76/3.64
	r(Cu−P_B)	2.32/2.35/2.32	2.29/2.31/2.27	2.30/2.29/2.24
	r(Cu−P_T)	2.25/2.27/2.23	2.29/2.30/2.28	2.26/2.32/2.28
	∠(P_B−Cu−P_B)	97/89/90	106/108/105	108/111/109
	∠(Cu−P_B−Cu)	83/90/91	74/72/75	72/69/71
	∠(P_T−Cu−P_T)	135/113/130	133/112/123	134/114/123
charge population[c]	Cu	0.67/0.57	0.69/0.59	0.70/0.58
	P_B	0.07/−0.65	0.20/−0.48	0.33/−0.25
	P_T	0.81/−0.07	0.83/−0.07	0.87/−0.05

[a] Units are Å (bond lengths) and deg (bond angles). P_B denotes bridging phosphorus atoms in the [Cu−P−Cu−P] core, while P_T denotes the ones outside of the core. [b] Geometrical parameter designations: theory (**X = 1**)/theory (**X = 2**)/experiment. Experimental geometries are from ref 22. [c] Charge population designations: theory (**X = 1**)/theory (**X = 2**).

changes may surely cause large geometric distortions in the molecule. Accordingly, we now turn our attention to the bonding interactions between the atoms in the [Cu−P−Cu−P] core.

3.2. Characterization of Bonding in the Diamond Core. Let us first consider the chemical bonding in the neutral species (**1** and **2**). One should expect some covalent character in the [Cu−P−Cu−P] diamond core on the basis of the diffuse nature of valence electrons of both Cu and P atoms and the fairly similar electronegativities of Cu and P. However, a Lewis picture of bonding in the core is not completely obvious when one considers the electron configurations of the Cu and P atoms. Because the valence shells of P atoms in the phosphide groups and Cu(I) atoms are completely filled ($3s^2 3p^6$ and $3d^{10}$, respectively), there will be no net bonding effect from the interactions between these orbitals. To answer this apparent paradox, a careful assessment of the chemical bonding will be required: is it simply 4 donor−acceptor interactions from P to Cu to satisfy the 18-electron rule or is some more novel covalency involved?

In principle, quantum chemistry calculations can accomplish such a purpose. Indeed, through quantum chemical assessment, Harkins et al. reported a peculiar bonding pattern in the highest occupied MO (HOMO) of the neutral species **1**, where p orbitals on bridging phosphorus atoms form a partial through-space bonding overlap mediated by copper d_{z^2} orbitals.[21] The shape of the HOMO is reproduced in Figure 3a. When we further calculated the Kohn−Sham orbital energy of the HOMO at various geometries, it showed a strong dependence on the geometrical distortions. This arises because partial through-space bonding overlap existing with a near-square core is lost as the angle ∠P_B−Cu−P_B becomes more obtuse as also shown in Figure 3a. At first glance, this fact appears to explain the geometric trends, since the neutral system prefers a longer Cu−Cu distance because the HOMO becomes more stable at that conformation with an increased bonding overlap.

However, such an argument cannot satisfactorily explain the preference for a particular square conformation, since, as shown in Figure 3c, the HOMO becomes monotonically more stable even at acute ∠P_B−Cu−P_B angles. More importantly, consideration of only the HOMO energy is inadequate. When one considers net bonding with canonical orbitals, one must take into account the canceling contributions of bonding and antibonding orbitals. Therefore, we must see whether lower energy MO's show opposing changes in orbital energy as a function of the core distortion. Indeed, the behavior of the HOMO-1 shown in Figure 3c exhibits exactly such behavior. We can see

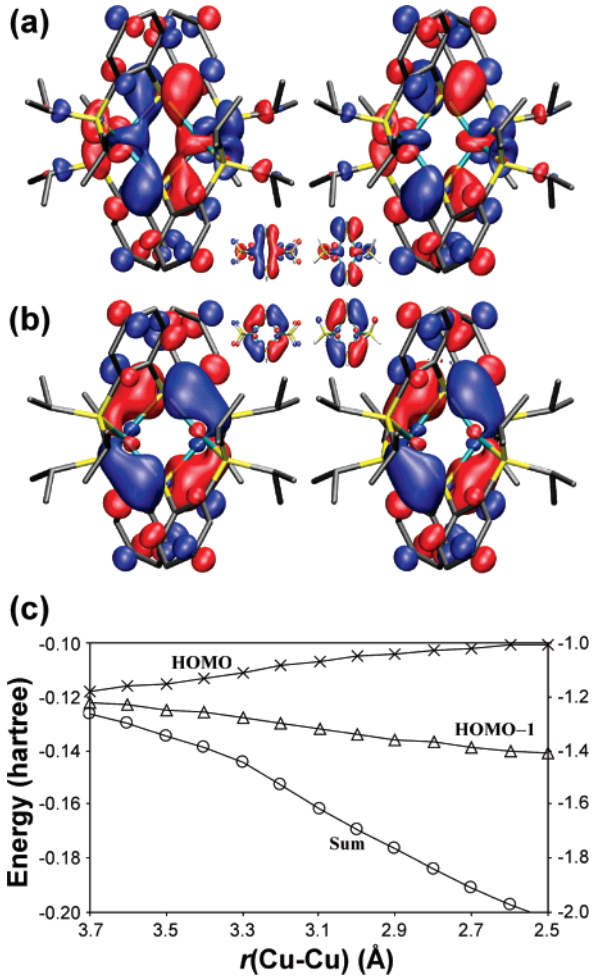

Figure 3. Shapes of the (a) HOMO and (b) HOMO-1 of **1** at the neutral geometry (left) and at the dicationic geometry (right) obtained at the BP86/D:T(2+)3P level of theory. The corresponding orbital shapes from the model molecule **2** are shown in the center. Atoms are color-coded as gray (C), yellow (P), cyan (Cu), and white (H). Hydrogens are not shown with **1** for simplicity. At the dicationic geometry, antibonding interactions from Cu d_{z^2} orbitals can be clearly seen in the HOMO, resulting in destabilization. (c) Kohn−Sham energy eigenvalues of HOMO and HOMO-1 as a function of Cu−Cu distance (left axis) on the basis of the results shown in Figure 2. Note that the equilibrium distance in **1** is ∼3.2 Å (left side), while the distance in $\mathbf{1}^{2+}$ is ∼2.6 Å (right side). The sum of Kohn−Sham orbital energies (right axis) in the occupied space is also presented to demonstrate that the geometrical preference of **1** is not a result of orbital stabilization/destabilization.

that the stability gain in the HOMO from longer Cu−Cu distances is compensated by loss of stability in HOMO-1. The

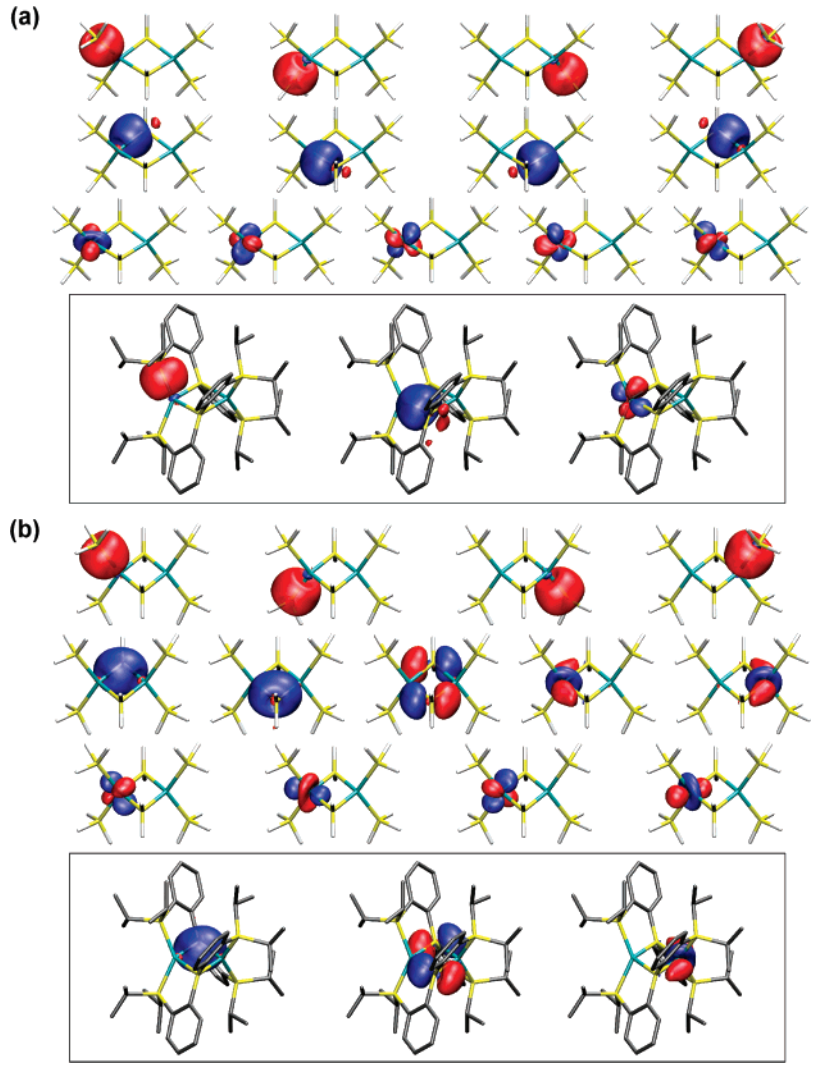

Figure 4. Localized valence occupied orbitals of (a) **1**/**2** and (b) $\mathbf{1}^{2+}$/$\mathbf{2}^{2+}$. In **2**, the orbitals can be classified as P_T−Cu bonding (top row), P_B−Cu bonding (middle row), and Cu nonbonding (bottom row), respectively. In $\mathbf{2}^{2+}$, the P_B−Cu bonding is drastically changed. Nonbonding orbitals on copper atoms (bottom rows) appear in a symmetrical fashion on both atoms and are shown only on the left side. P−H bonding orbitals are not shown to save space. The bonding in **1** and $\mathbf{1}^{2+}$ is quite similar to **2** and $\mathbf{2}^{2+}$, as can be seen for selected orbitals in the boxes. See Figure 3 for the atomic color codes.

simplified model molecule (**2**) also shows the same behavior in both the shapes and the energies of the orbitals.

In contrast, the localized orbitals are much more informative. In the neutral molecules (**1** and **2**), localization results in four classes of orbitals around the core: P−C/P−H bonding, P_T−Cu bonding, P_B−Cu bonding, and Cu nonbonding as presented in Figure 4a. The nonbonding Cu orbitals shown in the figure are clearly d-orbitals, suggesting that Cu 3d orbitals are not involved in the chemical bonding of this molecule. The shapes of the P−Cu bonding orbitals closely resemble combinations of the conventional sp^3-hybridized orbitals on both P and Cu atoms, and they are strongly polarized toward the P atoms. Accordingly, we describe bonding in the neutral molecule as donor−acceptor interactions from lone pairs on P atoms to vacant 4s and 4p orbitals of Cu atoms. Moreover, the preference for the square conformation in the core can be ascribed to the steric interactions of these four nearly equivalent P_B−Cu bonds. Back-donation from Cu (3d) to P is not likely because the empty 3d orbitals of P atoms are too high in energy for any effective coupling. Indeed, there is no appreciable back-donation from Cu observed in the localized orbitals shown in Figure 4a.

The nature of the bonding changes dramatically as the systems lose electrons upon oxidation. Because the monocations can be viewed as mixtures of the neutral and dicationic species, with their α-spin orbitals resembling the ones in the neutral species and their β-spin orbitals resembling the dicationic orbitals, we will only show the dication orbitals. After the electron extractions primarily from P_B atoms, they assume an sp^2-like electronic configuration (Figure 4b). With such a change, the electron donation from P_B to Cu is partly lost—the two remaining orbitals with this character are now sp^2 P_B lone pairs, and each of them connects to both Cu atoms in a 3-center donor−acceptor interaction. However, the p_x orbitals of P_B atoms with half-occupation become available as acceptor levels in the dicationic species. The corresponding donor orbitals are the Cu d_{z^2} orbitals as shown in Figure 4b, and this interaction will prefer obtuse $\angle P_B$−Cu−P_B angles. Because this new donor−acceptor interaction is more structure sensitive (due to the compact Cu d_{z^2} orbital) than the dative bond in the neutral, the monocation with half of this new interaction will be closer to the dication in its geometry. These findings appear consistent with previous experimental reports by Harkins et al.,[21] where the K-edge

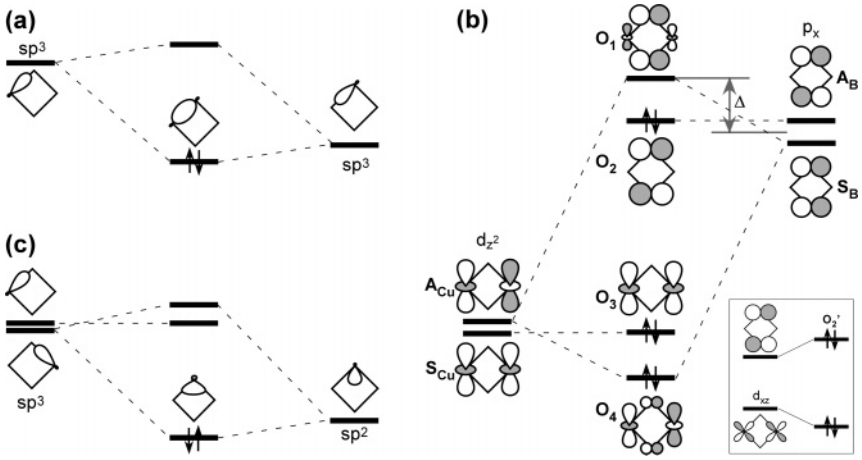

Figure 5. Schematic illustrations of important orbital interactions governing the bonding in the diamondoid core: (a) P → Cu dative bonding in the neutral; (b) covalent bonding in the dication; (c) dative bonding in the dication. In (b), △ represents the stabilization energy induced by the bond formation with Cu d_{z^2} and P_B p_x orbitals. The inset explains the interaction between O_2 and Cu d_{xz} orbitals, which is not crucial in the stabilization of the core. See text for detailed explanation of the interactions. Cu−Cu and P_B−P_B diagonal vectors define *x* and *z* axes, respectively. Radial nodes of 3p orbitals of P atoms are omitted for simplicity.

XAS[59] of P atoms showed growing covalent characteristics contributed by P_B 3p orbitals in the order of **1** < $\mathbf{1}^+$ < $\mathbf{1}^{2+}$. Their description of a π-bonding between P_B 3p's mediated by overlap with Cu 3d orbitals[21] is also in accord with our result.

On the basis of the above findings, we conclude that the peculiar plasticity of this diamondoid molecule arises from the significant change in bonding upon oxidations (P → Cu electron donation versus P ↔ Cu forward and back-donation). We note that these interesting characteristics must be caused by a delicate electronic balance between P and Cu atoms which changes with oxidation state. Formally, in the neutral species **1** and **2**, P_B atoms are negatively charged and rich in electrons. In reality, they will donate some electron density to adjacent positively charged copper atoms through weak dative bonds. After the P_B atoms each lose an electron in the oxidations, the copper atoms appear relatively richer in electrons. This new situation induces the copper atoms to share electrons with P_B atoms, via back-donation from the Cu d_{z^2} orbital, which is a driving force for geometric distortion. From the shape of this orbital, one can infer that the interaction will be more stable when the ∠P_B−Cu−P_B angle is large. Also, because the copper atoms use their electrons for back-donation to the P_B atoms, there is no direct metal−metal bond.

Let us summarize the localized picture of bonding in the dication relative to the neutral. Two oxidations on the $P_BR_2^-$ groups caused the loss of 2 P_B → Cu donor−acceptor interactions, so the Cu atoms are initially 16-electron and the P_B atoms are 7-electron. The two remaining P_B → Cu interactions become 3-center (Cu−P_B−Cu), thus enabling both Cu atoms to recover a formal 18-electron count. The odd electrons on the 2 P_BR_2 groups couple into an orbital with antibonding cross-ring interaction (an orbital explanation for why this is not the rather more obvious bonding interaction will be discussed in the following section). The two P_BR_2 groups gain a share in additional electrons through two 3-center Cu → P_B back-bonding interactions, which leaves them with more than a formal octet of electrons.

These features show interesting differences in comparison with the isoelectronic and structurally similar Cu_A center of cytochrome *c* oxidase, which has a [Cu−S−Cu−S] core. The Cu_A center is believed to have covalent character in its bonding,[16,60] and the present [Cu−P−Cu−P] system may be considered as an analogue of the Cu_A site.[21] At the same time, the Cu_A center exhibits some direct Cu−Cu interaction,[16,60] which is not found in [Cu−P−Cu−P]. This difference can be inferred from the substantially different Cu L_3-edge spectra for the two species (see refs 60 and 21). This contrast is especially interesting when we consider the apparent similarity in the cores of Cu_A and $\mathbf{1}^+$, which can be formally constructed with two $Cu^{1.5+}$ and two S^-/P^- from thiolate/phosphide. We attribute this discrepancy to a subtle difference in electronic properties of sulfur and phosphorus. Considering the larger electronegativity of S, the effective oxidation on copper atoms will likely be larger in Cu_A, and the formation of a direct bond using a hole in the Cu(II) atom will be promoted. The difference will be more pronounced in a Cu_2O_2 system,[61−63] where the ligand electronegativity is increased and the metal−ligand bonding is less covalent. Various differences found in another analogue with a Cu_2N_2 core reported by Peters and co-workers[21,64,65] are likely caused by a similar change in the electronic structure.

3.3. Orbital Interactions. We can rationalize the form of the localized orbitals in the diamondoid core presented above, in terms of a simplified orbital interaction diagram,[66] even though the overall orbital interactions are necessarily quite complicated due to the electron-rich nature of the transition metal atoms. We first briefly consider the neutral species, where our zero-order atoms are positively charged Cu(I) ($3d^{10}$) and negatively charged phosphide, with 2 lone pairs. As we previously saw in Figure 4a, each Cu atom participates as an acceptor via its empty 4sp orbitals (hybridized as sp^3), in 4 dative

(59) Solomon, E. I.; Hedman, B.; Hodgson, K. O.; Dey, A.; Szilagyi, R. K. *Coord. Chem. Rev.* **2005**, *249*, 97.
(60) DeBeer George, S.; Metz, M.; Szilagyi, R. K.; Wang, H.; Cramer, S. P.; Lu, Y.; Tolman, W. B.; Hedman, B.; Hodgson, K. O.; Solomon, E. I. *J. Am. Chem. Soc.* **2001**, *123*, 5757.
(61) Kitajima, N.; Moro-oka, Y. *Chem. Rev.* **1994**, *94*, 737.
(62) Cramer, C. J.; Kinal, A.; Wloch, M.; Piecuch, P.; Gagliardi, L. *J. Phys. Chem. A* **2006**, *110*, 11557.
(63) Cramer, C. J.; Wloch, M.; Piecuch, P.; Puzzarini, C.; Gagliardi, L. *J. Phys. Chem. A* **2006**, *110*, 1991.
(64) Harkins, S. B.; Peters, J. C. *J. Am. Chem. Soc.* **2004**, *126*, 2885.
(65) Harkins, S. B.; Peters, J. C. *J. Am. Chem. Soc.* **2005**, *127*, 2030.
(66) Hoffmann, R. *Acc. Chem. Res.* **1971**, *4*, 1.

interactions with 4 neighboring P atoms. Thus, the 18 electron rule is satisfied and the filled Cu(3d) orbitals do not participate in bonding. The 4 donor−acceptor interactions within the ring are as cartooned in Figure 5a and are polarized toward the P atoms.

The more interesting and complex case is the dication, corresponding to the orbital interaction diagram shown in Figure 5b. The zero-order picture of the atoms is that the double ionization converts closed-shell phosphide anions $(P_BR_2)^-$ to neutral radicals $(P_BR_2)^\bullet$. The appropriate hybridization of the P_B atoms is now sp^2, and the radical electron in an in-plane p_x orbital will play an important role. First, through-space coupling of the two p_x orbitals generates two levels, one symmetric and occupied (S_B) and one antisymmetric and empty (A_B), with very small splitting (right column in Figure 5b), because the overlap of the p_x orbitals is poor. At the same time the lone pair sp^2 orbital on each P_B can form a delocalized dative bond with the 2 Cu atoms, as cartooned in Figure 5c. Relative to the neutral, the dication has lost 2 of the 4 dative bonds within the ring and attained a weak direct interaction between the 2 P_B atoms, described by the S_B orbital, to this stage.

The story is still far from complete because the very small splitting between bonding and antibonding interactions between P_B atoms can be significantly perturbed by coupling to neighboring groups, since it is easy to perturb a small splitting. The neighboring groups within the ring are the Cu atoms, and they have filled 3d levels of which the d_{z^2} orbitals can interact with the S_B orbital. The two Cu d_{z^2} orbitals form a similar pair of symmetry-adapted combinations, S_{Cu} and A_{Cu} with even smaller splitting (left column in Figure 5b), at lower energy. S_B can couple to A_{Cu}, giving perturbed antibonding (O_1) and bonding (O_4) levels. A_B and S_{Cu} do not have the correct symmetry to interact further and are therefore not additionally perturbed, becoming the final O_2 and O_3 levels. Interestingly, the initial energy ordering of in-phase and out-of-phase mixtures of $P_B(p_x)$ orbitals (i.e., $S_B < A_B$) has been *reversed* by the neighboring group interactions (second column in Figure 5b). The net result is that O_3 and O_4 are relatively low in energy (both occupied) while O_1 and O_2 are high in energy with a relatively small gap (half-occupied).

These two highest energy symmetry-adapted orbitals (O_1 and O_2) are similar to the HOMO and HOMO-1 of the neutral system presented in Figure 3. In the dication, only three orbitals are occupied (O_2, O_3, and O_4). The resulting bonding effect (energy stabilization with respect to the isolated fragments as we have defined them) is represented by Δ in Figure 5b. Furthermore, this picture is in exact accord with the localized orbitals (except that the lower energy occupied levels, O_3 and O_4, are linearly combined to promote localization: L_1, $\sim(O_3 + O_4)/\sqrt{2}$; L_2, $\sim(O_3 - O_4)/\sqrt{2}$). In the neutral state, all four orbitals will be occupied, and localization of these orbitals will lead them back to the primitive atomic orbitals by appropriate orbital rotations.[67] In this case, the net bonding (from differently charged fragments) results from electron donation from P_B atoms to empty Cu orbitals as already explained with Figure 5a.

Of course, this simple picture has omitted many less important interactions between Cu d and P_B p orbitals. Perhaps the next most important one will be the interaction involving Cu d_{xz} orbitals. A symmetry-adapted mixture of d_{xz} orbitals (shown in the inset of Figure 5b) and O_2 have the same symmetry and can directly interact with each other, to form linear combinations in a more complete description. In fact, the shape of the HOMO-1 shown in Figure 3 clearly exhibits this character. However, because there is no orbital energy crossing between the HOMO and the HOMO-1 as shown in Figure 3, the two orbitals generated by mixing of O_2 and d_{xz} will both be filled, and there will be no net bonding interaction from this coupling. Again, this is in accord with the depiction given by the localized orbitals, where Cu d_{xz} orbitals appeared as nonbonding.

3.4. Emergence of a Singlet Diradicaloid from Two Oxidations. In previous sections, we have seen that successive oxidations of the diamondoid molecule extract electrons mostly from P_B atoms and its adjacent surroundings. In the dication, this process leaves the system with two spatially separated (and thus partly unpaired) electrons (or holes). Consequently, the dication of this diamondoid species is likely to have diradicaloid[24−27] character. If the two unpaired electrons in such a state occupy two degenerate orbitals, the system will likely have a triplet ground state (Hund's rule[68]). This degeneracy would certainly happen if there were no orbital interactions between the two P_B atoms. Molecular magnets with dinuclear transition metal centers[69] will be close to this no orbital interaction limit. However, in the previous section we discussed both weak through-space interactions and stronger through-bond interactions that make the situation richer in the present system. Indeed, we have seen that the calculated singlet ground state is always lower in energy than the lowest triplet state for the dicationic system (from Figure 2). Thus, the ground state appears to be singlet, with the orbital interactions causing sufficient perturbations to favor the singlet state over the triplet state to violate Hund's rule.[24,25,70] We now investigate the extent to which it is diradicaloid with further calculations and compare its characteristics against other experimentally isolated (and thus stable) singlet diradicaloids.[71−76]

As discussed in Methods, perfect pairing (PP) calculations are the tool we use to explore this issue. In both $\mathbf{1}^{2+}$ and $\mathbf{2}^{2+}$, we have found one strongly correlated active orbital pair with the antibonding occupation number reaching up to ∼0.4 electrons. (See Supporting Information for the detailed occupation numbers of the frontier orbitals.) The shapes of these optimized orbitals are presented in Figure 6.[77] Interestingly, this pair possesses different characteristics (nonbonding and antibonding) compared to the orbitals in a singlet diradicaloid B_2P_2 ring (bonding and antibonding), which was recently synthesized by Bertrand and co-workers[73] and subsequently characterized by various research groups.[74−76] This may seem surprising when one considers their seemingly similar core structures ([Cu−P−Cu−P] versus [B−P−B−P]). However, the major atomic

(67) Helgaker, T.; Jørgensen, P.; Olsen, J. *Molecular Electronic-Structure Theory*; Wiley: New York, 2000.
(68) Kutzelnigg, W. *Angew. Chem., Int. Ed. Engl.* **1996**, *35*, 573.
(69) Ceulemans, A.; Chibotaru, L. F.; Heylen, G. A.; Pierloot, K.; Vanquickenborne, L. G. *Chem. Rev.* **2000**, *100*, 787.
(70) Kollmar, H.; Staemmler, V. *Theor. Chim. Acta* **1978**, *48*, 223.
(71) Jung, Y.; Head-Gordon, M. *J. Phys. Chem. A* **2003**, *107*, 7475.
(72) Jung, Y.; Head-Gordon, M. *ChemPhysChem* **2003**, *4*, 522.
(73) Scheschkewitz, D.; Amii, H.; Gornitzka, H.; Schoeller, W. W.; Bourissou, D.; Bertrand, G. *Science* **2002**, *295*, 1880.
(74) Cheng, M.-J.; Hu, C.-H. *Mol. Phys.* **2003**, *101*, 1319.
(75) Seierstad, M.; Kinsinger, C. R.; Cramer, C. J. *Angew. Chem., Int. Ed.* **2002**, *41*, 3894.
(76) Shoeller, W. W.; Rozhenko, A.; Bourissou, D.; Bertrand, G. *Chem.—Eur. J.* **2003**, *9*, 3611.
(77) In comparative calculations of the neutral molecules, the antibonding occupations are found to be less than 0.04 electrons. Thus, the diradical character is specific to the dications.

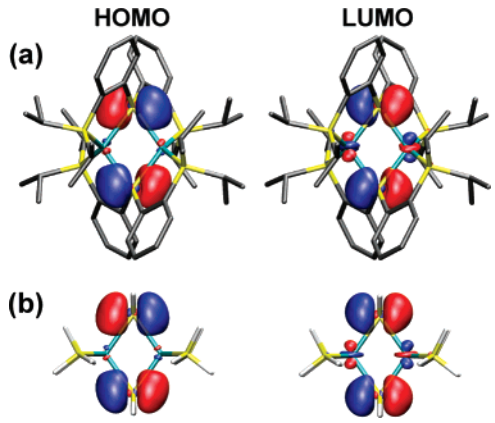

Figure 6. Most strongly correlating active pairs of orbitals obtained with perfect pairing optimizations for (a) $\mathbf{1}^{2+}$ and (b) $\mathbf{2}^{2+}$. The atomic color codes are as in Figure 3.

orbitals contributing to the diradicaloid formation, in-plane p_x orbitals on P atoms in [Cu−P−Cu−P] versus out-of-plane p_z orbitals on B atoms in [B−P−B−P], are fundamentally different, and as a result, the nature of the interacting orbital pairs becomes dissimilar. For example, from Figure 2 of ref 73, one can observe a noticeable amount of direct interaction between the two boron atoms in [B−P−B−P], while there is only an indirect interaction between P atoms mediated by Cu in [Cu−P−Cu−P] (Figure 4). The larger sizes of the copper atoms in [Cu−P−Cu−P] will also contribute to the differences in the orbital interactions.

If the gap between nonbonding HOMO and antibonding LUMO ([Cu−P−Cu−P] case) is smaller than the gap between bonding HOMO and antibonding LUMO ([B−P−B−P] case), we can further hypothesize that the present system will have stronger static electron correlation induced by the interacting orbital pair. Since an exactly half-occupied degenerate orbital pair would have antibonding occupation of 1 electron and be an idealized 100% diradical, we can say that this molecule has a diradical character that approaches 35−40%. This is approximately twice the extent of diradical character calculated previously for the [B−P−B−P] system,[71,72] which is a very significant difference. Experimental evidence supports this hypothesis: the vertical gaps of the two lowest singlet states (S_0 and S_1) as measured by the ultraviolet/visible (UV/vis) absorption peaks are 680 nm (1.8 eV) for [Cu−P−Cu−P][22] and 446 nm (2.8 eV) for [B−P−B−P],[73] respectively, supporting that the degree of static correlation is actually larger in [Cu−P−Cu−P]. In addition, theoretical estimation of the triplet/singlet (T_1/S_0) gap[78] for [Cu−P−Cu−P] is estimated to be significantly smaller than that of [B−P−B−P] (∼16 kcal/mol versus ∼27 kcal/mol[72]) when calculated with spin-flip time-dependent DFT.[71,72,79,80] Further comparative studies with different substituents can be expected to tune the orbital interactions and potentially either stabilize the singlet state (reduce diradical character) or destabilize the singlet state (by increasing diradical character).

4. Concluding Remarks

In summary, we have shown that a change in the character of Cu−P bonds in the core of the diamondoid molecule is the driving force for the drastic geometry changes upon oxidations. Because the changing bonds primarily involve core atoms in the diamondoid rather than remote substituents, a small model molecule with truncated ligands could reproduce the same geometric aspects. The nature of the bonds was inspected through the use of localized orbitals. In the neutral state, the bond was dominated by dative bonds from phosphorus atoms to Cu(I) atoms. When the molecule is oxidized, the bridging phosphide groups lose electrons. This opens a vacancy in the valence, which is partially stabilized by back-donation from copper d-orbitals. The large geometry change was ascribed to this new bond formation. On the basis of an orbital interaction picture, we expected that the dicationic system may have significant singlet diradicaloid character. Perfect pairing calculations suggest as much as 35−40% diradical character on a scale set by the occupation of the LUMO. These findings satisfactorily explain various experimental observations such as ^{31}P NMR and strongly red-shifted electronic absorption (600−800 nm) of the dication.[21,22]

All these interesting features are related to the nature of the bonding within the [Cu−P−Cu−P] core. The close reproduction of various chemical properties from the use of a simplified model molecule suggests that the ligand "side chains" do not play an important role in the redox properties of this molecule. Qualitatively, this is in accord with various findings for closely related Cu−S systems, where the redox behavior is determined by covalent Cu−S bond(s)[13,15,16,19] and the coordination geometry is not strained by the surrounding ligand groups.[18] However, the apparent difference with the Cu_A center of cytochrome *c* oxidase (no metal−metal bond in [Cu−P−Cu−P]) suggests that the chemical properties of the metal center (and the core) can be delicately tuned by changing the interaction between the metal and the ligand and the properties of the bridging atom. In fact, we should consider that such tuning is what Nature has optimized with various enzymes involving copper and sulfur atoms. With the variety of bridging atoms (N, O, S, and P) together with the additional ability to fine-tune their electronic properties through ligand side chain substitutions, one may anticipate further exploration of interesting related molecules. Synergistic efforts using both theory and experiment will be valuable in such developments.

The appearance of diradical character is also intriguing for various reasons. Because diradicaloids are often important intermediates and transition states in various biological processes, designing molecules with large diradicaloid character may help to better understand such processes. In addition, diradicaloids have potential usefulness in developing novel molecules such as spintronic materials and molecular ferromagnets. We consider the diradicaloid character in [Cu−P−Cu−P] to be interesting and unusual for two reasons. First, while it is relatively common for dinuclear transition metal centers[69] to have unpaired electrons which couple antiferromagnetically, this interaction is usually indirect. Thus while there is often high diradical character, the associated coupling between the two electrons is very weak. In [Cu−P−Cu−P], the coupling is significant (singlet−triplet gap of ∼16 kcal/mol), yet the diradical character is unusually high. Second, in most transition

(78) In the limit of 100% diradical, triplet and singlet ground states become degenerate when the spin−orbital coupling is ignored. Thus, a small triplet/singlet gap can be considered as a good indicator of the degree of diradical character.
(79) Shao, Y.; Head-Gordon, M.; Krylov, A. I. *J. Chem. Phys.* **2003**, *118*, 4807.
(80) Krylov, A. I. *Chem. Phys. Lett.* **2001**, *338*, 375.

metal systems the coupled electrons are primarily associated with the metal sites. In this system, remarkably, the coupled electrons largely reside on the ligand sites. We expect that computational and experimental studies of derivatives related to the present system will be of considerable interest in these respects.

Acknowledgment. This work was supported by grants from the Department of Energy (through the SciDac and Computational Nanosciences Programs) with additional support from British Petroleum through the MC^2 program.

Supporting Information Available: Complete ref 53 citation, comparisons of all-electron BP86 potential energy surface with all-electron B3LYP and relativity-corrected effective core BP86 surfaces, a brief explanation of the adequacy of using local orbitals, detailed PP occupancy data of the dications, a plot of diradical character versus Cu−Cu distance, and all coordinates and energies of structures represented in Table 2. This material is available free of charge via the Internet at http://pubs.acs.org.

JA0764916